LARGE SCALE GLOBAL STRUCTURAL CHANGES OF THE PURPLE MEMBRANE DURING THE PHOTOCYCLE

JAMES E. DRAHEIM AND JOSEPH Y. CASSIM
Department of Microbiology and Program in Biophysics, College of Biological Sciences, The Ohio State University, Columbis, Ohio 43210

ABSTRACT Both the solution and the oriented film absorption and circular dichroic spectra of the bacteriorhodopsin (bR_{568}) and M_{412} intermediate of the purple membrane photocycle were compared over the wavelength region 800–183 nm to assess structural changes during this photocycle. The main findings are (*a*) loss of the excitonic interaction among the chromophoric retinal transitions indicating disordering of the retinal orientations in the membrane and distortions of the membrane hexagonal crystal lattice, (*b*) structural change of the chromophoric retinal, (*c*) changes in the key interactions between the retinal and specific groups in the local environment of the apoprotein, (*d*) significant changes of the tertiary structure of the bR with negligible secondary structure involvement, and (*e*) a net tilting of the rodlike segments of the bR polypeptides away from the membrane normal. These findings are in accord with large scale global structural changes of the membrane during the photocycle and with structural metastability of the bR molecules. An important implication of these changes is the possibility of transmembrane retinal-regulated pulsating channels during the photocycle. The significance of this possibility in respect to models for the proton translocation function of this membrane is discussed.

INTRODUCTION

One outstanding problem in bioenergetics is how protons are transported across hydrophobic bilayers of membranes. Over the last decade research on this problem has increasingly been focused on the purple membrane, PM, of the *Halobacterium halobium* because of the relative simplicity of its structure and function (for comprehensive reviews see references 1 to 6). The PM is a specialized membrane domain of the plasma membrane of the bacterium. It contains a single protein species, bacteriorhodopsin (bR), which constitutes ~75% of the membrane's dry weight with the remainder being lipids. BR is a chromoprotein to which retinal is bound by a protonated Schiff-base linkage.

The bR consists of a single polypeptide chain of 248 amino acids with a molecular weight of 26,534 daltons. The primary structure of the protein has been determined (7, 8). The secondary structure of the protein is highly α-helical but may contain appreciable amounts of β-pleated sheet (9). The tertiary structure of the protein can be approximated by the polypeptide folded back and forth on itself, forming seven rodlike structural segments oriented nearly perpendicular to the membrane plane. The protein molecules are packed as cyclic trimers forming a hexagonal crystal lattice resulting in a highly rigid and ordered membrane structure (10).

Address all correspondence to Dr. J. Y. Cassim.

Upon illumination, the chromophoric retinals of the bRs undergo a photocycle resulting in the formation of several transient photointermediates that have been characterized by their different absorption spectra. There have been attempts to correlate this photoprocess with the light-induced vectorial translocation of protons across the PM, which is essential to the anaerobic ATP synthesis process of the halobacterium. The relatively long-lived intermediate termed M_{412} has been of particular interest in this regard since the Schiff-base linkage between the retinal and the apoprotein is deprotonated and reprotonated during its formation and decay, respectively (11). Furthermore, there may be a change of the retinal from the all-*trans* to 13-*cis* configuration during this process (12). Although numerous studies of this photocycle have been reported, most research has been focused on the role of the retinal. The nature and the extent of the structural change of the apoprotein during this process still remains poorly understood in spite of its apparent importance to the mechanism of proton translocation. In fact, it has been assumed that large scale conformational changes of the protein are a priori unlikely because of the crystallinity of the membrane structure and the apparent absence of large changes in the retinal orientations during the photocycle (4).

To rectify this lack of information concerning the protein action during the photocycle, the comparative absorption and circular dichroic, CD, spectra of the light-adapted form, bR_{568}, and the M_{412} photointermediate of the PM in

solution and oriented in a film were studied over the wavelength range of 800 to 183 nm. The spectra were analyzed according to methods developed by this laboratory over the last decade (13–16). Results are in accord with large scale global structural changes of the PM during the bR_{568} to M_{412} transformation in the photocycle and with inherent structural metastability of bR molecules. Important findings are the loss of the excitonic coupling among the chromophoric retinals of the PM and the net tilting of the polypeptide segments of the protein. An important implication of these findings is the possibility of formation of retinal-regulated pulsating channels during the photocycle. Furthermore, it is shown that these results are more consistent with regulated channel or deformation wave models for proton transport in membranes than with the current popular semiconductor or ice models.

MATERIALS AND METHODS

The PM was isolated from the *Halobacterium halobium* S9 mutant according to the procedures of Becher and Cassim (17). Absorption and CD spectra were recorded with a Cary 118C spectrophotometer with far ultraviolet (UV) modification and a scattered transmission accessory and a Cary 60 spectropolarimeter with 6003 CD attachment, respectively (Varian Associates, Inc., Instrument Group, Palo Alto, CA), as previously described in detail (13). The cryostats used for low-temperature spectral measurements were specially designed quartz optical cell Dewars based on the cold finger principle (Kontes-Martin, Evanston, IL). The temperature was maintained at −70°C with a dry ice-ethanol bath.

In the solution studies, the PM was completely transformed into the M_{412} species in a 5.1 M NaCl solution titrated to pH 10 with 0.1 M NaOH and then mixed with two parts of spectral grade glycerol (18). However, for far UV studies to avoid excessive absorbances it was necessary to lower the NaCl concentrations to 0.33 M. The membrane protein concentration was also adjusted so that the concentration ratio of protein to NaCl remained unchanged. Conversion was achieved by exposing the solution to light focused from a 500-W DAY-DAK projector lamp (GTE Products Corp., Winchester, KY) and filtered through 3.2 cm of $CuSO_4$ solution and a yellow Corning 500-nm high-pass glass filter (Corning Glass Works, Corning Science Products, Corning, NY) while slowly lowering the temperature of the solution to −70°C and maintaining it at this temperature. The M_{412} species formed was stable at this temperature for long periods of time. It was found that the intensity of the measuring light of the Cary 60 spectropolarimeter (Varian Associates, Inc.) was of sufficient strength to cause photoselection by markedly back converting the M_{412} to the bR_{568} species during normal recording of the PM CD spectra. Repeated recordings created a steady state mixture of the two optical species in the cell. Photoselection was avoided by measuring the ellipticity point by point. After each single wavelength measurement the PM was exposed to the spectropolarimeter light at 560 nm for 10 min with the slits maximally open to correct for any back converting of the M_{412} species. This procedure was only necessary in the visible region. Photoselection was not observed during near or far UV recordings. Nor was it observed during absorption measurements with the Cary 118 C spectrophotometer (Varian Associates, Inc.) at any wavelength indicating that the measuring light of this instrument is not of sufficient strength to cause any observable photoselection.

For oriented PM studies, well-oriented PM films were formed by layering 1 cc of PM solution (OD_{568} = 0.5–1.8), which was previously filtered, degassed, and adjusted to pH 9.0 with 0.1 M NaOH, onto optical quality flats of Suprasil-S quartz (Precision Cells, Inc., Hicksville, NY). The PM solution was then slowly dried at low humidity in a desiccator with a beaker of saturated $LiCl_2$ solution. After formation, the film was incubated at high humidity in a desiccator with a beaker of saturated K_2SO_4 solution for at least 24 h. During spectral measurements, care was taken to maintain the film in a hydrated state by sealing the film in a specially designed optical cell. The quality of the films was maintained according to our previously published criteria (15).

Maximum transformation from bR_{568} to M_{412} was achieved in films by illuminating a hydrated film for 15 min at ambient temperature with the filtered 500-W DAY-DAK projector light (GTE Products Corp.). Then the temperature of the film was slowly decreased to −70°C and maintained at this temperature for another 15 min while continually illuminating the film. A maximum conversion of ~80% was achieved by this method and could be maintained for long lengths of time at −70°C. However, maximum transformation was possible only with fresh membrane preparations. Similar conversions were also achieved for thinner films (0.01–0.02 absorbance) by illuminating directly with the measuring light of the Cary 60 spectropolarimeter (Varian Associates, Inc.) with the monochromator set at 560 nm and the slits maximally opened. No photoselection was observed in oriented films in any wavelength region at the recording speeds used.

Linear dichroism was measured as previously described in detail (19). For homogenous orientations of the chromphoric retinal the appropriate relationship used for determining the out-of-plane angle ϕ of the retinal is

$$D = \frac{A_H}{A_V} = 1 + \frac{1}{n^2}(2\tan^2\phi - 1)\sin^2\alpha,$$

where D is the dichroic ratio, A_H and A_V are the absorbance of horizontally and vertically polarized light, respectively, n is the index of refraction of the PM, ϕ is the angle of the transition dipole moment of the retinal with respect to the membrane plane, and α is the angle between the plane of the optical flat and the incident light. In the present study, α was set at 25° and n was assumed to be 1.53 for the visible wavelengths. For heterogenous orientations of the retinal the relationship becomes

$$D = 1 + \frac{1}{n^2}\left(2\frac{\sum_i \sin^2\phi_i}{\sum_i \cos^2\phi_i} - 1\right)\sin^2\alpha.$$

RESULTS AND DISCUSSIONS

Visible Spectra

In Fig. 1 the visible absorption spectrum of a PM solution of the stabilized M_{412} photointermediate is compared with that of the light-adapted species, bR_{568}, under the same conditions. As previously shown, transformation to the M_{412} species results in a shift of the wavelength maximum from 568 to 412 nm with a decrease in extinction. Furthermore, spectral fine structure is evident in the band of the M_{412} species in sharp contrast to that of the bR_{568} species (20). The appearance of the fine structure in the spectrum of the M_{412} species may be attributable to spectral contributions from the vibrational structure of the retinal, which become more resolved during the species transformation due to a change in the retinal from a more twisted configuration to a more planar one. Although similar fine structure is present in the spectra of PM with reduced retinal, retro-retinal, it has been shown that it is not very probable that the retinal of M_{412} has a retro-structure (21). Another explanation is that M_{412} is not a single optical

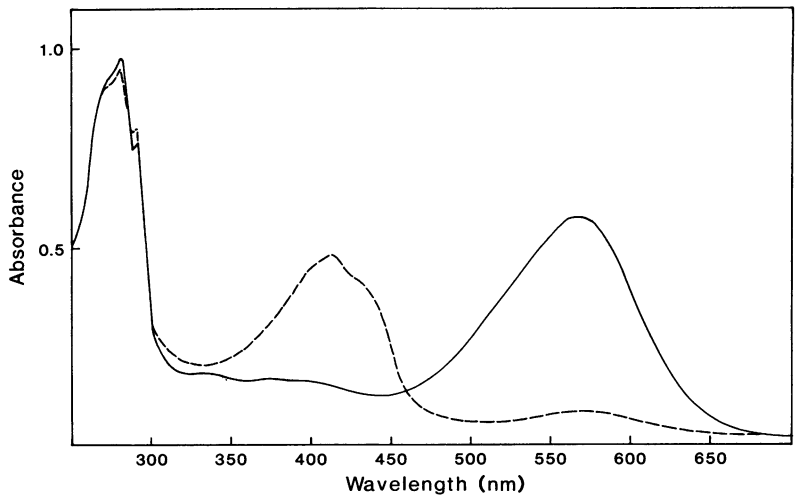

FIGURE 1 Comparative solution absorption spectra of the bR_{568} species (—) and M_{412} species (---) of the purple membrane in the visible and near UV regions in a 5.1 M NaCl solution titrated to pH 10 and then mixed with two parts of glycerol. Optical pathlength was 1 mm and the membrane protein concentration was 79.4 μM. Temperature was −70°C.

species but a mixture of several species with slightly different absorption spectra and that the observed spectrum is a resultant of these spectra.

The solution CD spectra of the two species under the same conditions used for the absorption studies is compared in Fig. 2. It is apparent that the CD band patterns of the two species are very different. The nonconservative biphasic bands of the bR_{568} species centered ~568 nm have been replaced by a relatively large positive band with fine structure, which seems to be a reflection of the absorption band of the M_{412} species shown in Fig. 1. There is also a relatively very small negative band at ~450 nm. The absence of measurable optical activity in the M_{412} CD spectrum at wavelengths >500 nm indicates complete species conversion. The small extinction at 568 nm remaining in the M_{412} absorption spectrum is probably due to residual carotenoids in the PM that are not optically active.

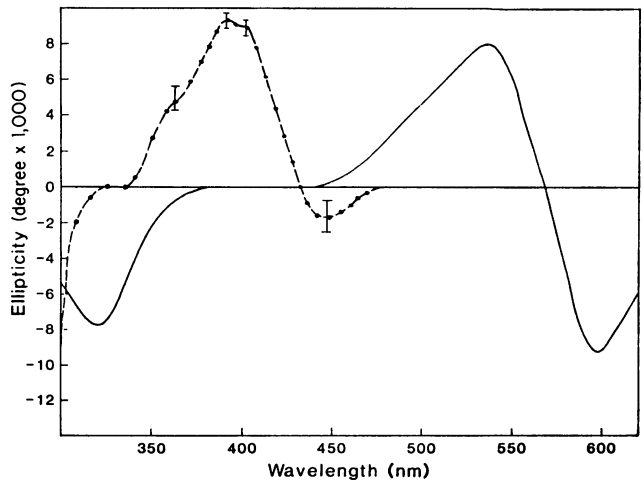

FIGURE 2 Comparative solution circular dichroic spectra of the bR_{568} species (—) and M_{412} species (---) of the purple membrane in the visible region under the same conditions used for the absorption spectra of Fig. 1. A portion of the spectrum of M_{412} species was measured point by point as indicated by data points with error bars to prevent photoselection.

Currently, two short communications have appeared on the solution CD of the M_{412} species with conflicting results (22, 23). In neither study was there a complete species conversion as indicated by the published spectra. Furthermore, it is apparent that the spectra of both these studies were distorted by artifacts due to photoselection, to problems associated with photoreactions induced by the measuring light, and to poor spectral resolution due to the recording procedures used. Although the negative CD band was resolved in the spectrum of Heyn et al. (22), distortions resulted in conservative amplitudes. On the other hand, Yoshida et al. (23) failed to observe the negative band. Also, neither group succeeded in resolving the fine structure of the CD band. In the present study, photoselection was circumvented without the loss of spectral resolution by using point-by-point measurements. The resolution of the fine structural details of the absorption band in the CD band is an indication of the accuracy of the present determination of this band. Since the transitions responsible for the absorption and CD bands are the same, the origins of the fine structure of the CD band should be the same as ones discussed for the absorption band.

The interpretation of the bR_{568} biphasic CD bands is crucial to the analysis of the CD bands of the M_{412} in respect to the structural changes resulting from the species transformation. It has been shown that the shapes of these biphasic bands can be explained most simply in terms of excitonic interactions among the retinals (13, 15, 16, 24). Considering the geometric organization of the retinal molecules in the PM, excitonic interactions should give rise to conservative biphasic CD bands with a crossover wavelength at the absorption maximum of the chromophoric

retinal. The observed nonconservative profile is the resultant of these excitonic bands and a monomeric Gaussian band. The monomeric band arises from the induced asymmetry of the retinal in the environment of the apoprotein and is centered at the same wavelength as the absorption band. The sign of this monomeric band varies with different conditions. Therefore, the overall shape of the nonconservative biphasic bands is due to the sign of this monomeric band. The predominant negative lobe of the bR_{568} biphasic band in Fig. 2 is due to the fact that the monomeric band is negative in glycerol (25). This is in contrast to the predominant positive lobe usually observed in aqueous solutions at neutral pH in which the monomeric band is positive (15). Recently there has been evidence that the excitonic interactions among the retinals must be of the weak-coupling type rather than strong-coupling type as first assumed (26). This will significantly effect the energy transfer time by this process but not the overall contributions to the CD spectra. Furthermore, weak-coupling excitonic interactions are expected to result in a rate of excitonic energy transfer that is much slower than that of the photocycle.

The profile of the M_{412} CD spectrum shown in Fig. 2 does not seem to be in accord with significant excitonic contributions to the optical activity of this species. However, excitonic contributions to the spectrum cannot be completely ruled out based only on this spectrum. Application of the formalism of the exciton theory to the molecular geometry of the PM indicates that if the plane of the PM is oriented perpendicular to the incident light, symmetry considerations require that all excitonic contributions to the CD spectrum must vanish (15). Such an orientation of the PM is achieved during film spectral studies. Therefore, if there is significant excitonic contributions to the spectra, the shapes of the film CD bands should be distinctly different from the solution ones. However, the differences in absorption bands should be minimal since the in-plane excitonic transitions are almost completely allowed at the expense of the out-of-plane excitonic transition due to the orientation the chromophoric retinal (15). The film absorption and CD spectra in which the spectra of the M_{412} species are compared with those of the bR_{568} species are shown in Figs. 3 and 4, respectively. The maximum species conversion that was possible in films was 80%. To facilitate comparisons of the two spectra, the spectrum of M_{412} extrapolated to complete conversion is also shown. It is clear that the shapes of the M_{412} film absorption and CD bands are similar to those of the solution bands. Furthermore, the spectral fine structure present in the solution spectra is also present in the film spectra of the M_{412} photointermediate. This is in sharp contrast to the spectra of the bR_{568} in which only the shapes of the absorption bands are nearly the same. The shapes of the CD bands are drastically different. Therefore, in view of these results the excitonic contribution to the spectra of the PM must vanish as a consequence of the bR_{568} to M_{412} species transformation.

Since it is clear that the small negative CD band of M_{412} at ~450 nm cannot be assigned to excitonic contributions and has no counterpart in the bR_{568} spectra, one possible explanation may be that this band is due to a low-energy n-π^* transition of the chromophore. If the retinal-lysine Schiff-base linkage is unprotonated, a nonbonding orbital of the Schiff-base nitrogen is possible. It has been suggested that bR_{568} transformation to M_{412} involves deprotonation of the retinal-lysine Schiff-base linkage (11). Based on symmetry considerations, the n-π^* transition is electric-dipole forbidden. However, rotatory strength can be generated by a mixing of electronic states by the asymmetric charge environment of the apoprotein. This CD band may provide an independent probe of the protonation state of the chromophoric Schiff-base nitrogen.

This apparent loss of excitonic contributions to the CD spectrum must be a reflection of a global change in the PM

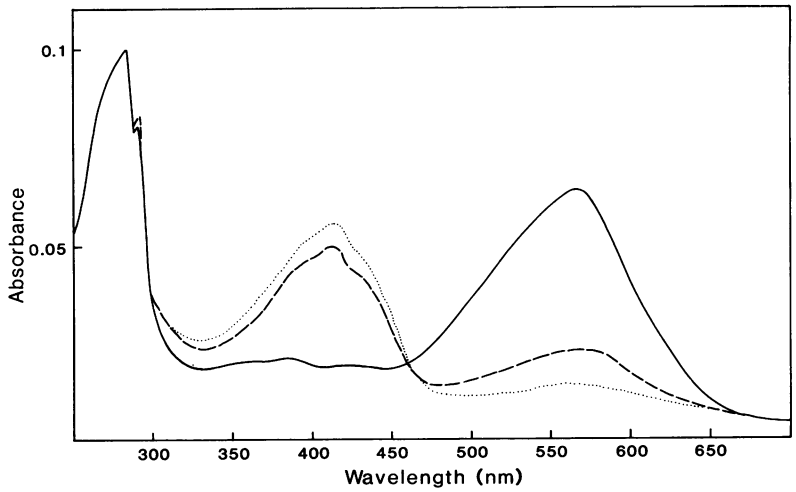

FIGURE 3 Comparative film absorption spectra of the bR_{568} species (—), M_{412} species at 80% conversion (---), and M_{412} species extrapolated to complete conversion (· · ·) of the purple membrane in the visible and near UV regions. Temperature was −70°C.

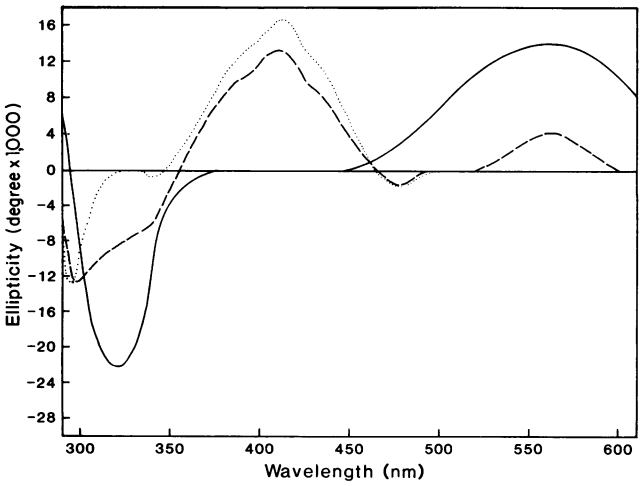

FIGURE 4 Comparative film circular dichroic spectra of the bR_{568} species (—), M_{412} species at 80% conversion (---), and M_{412} species extrapolated to complete conversion (• • •) of the purple membrane in the visible region. Temperature was −70°C.

structure in view of the strong dependency of this phenomenon on molecular geometry. These changes may be in the chromophoric position or in the order of the chromophoric positions in the membrane crystal lattice or both. The rotatory strength due to excitonic interactions is dependent on the in-plane and out-of-plane orientations of the chromophoric transition dipole moments (27). For certain orientations of the transition dipole moments, the rotatory strengths of the excitonic transitions will be zero. For example, in terms of the angular orientations of the transition dipole moments, this will occur when the moments are confined to the PM plane. Since the out-of-plane orientation angles of the retinals are ~20° to 24° in the bR_{568} species, this would indicate a drastic change in the retinal positions during the transformation to the M_{412} species (2). However, based on the results of linear dichroic measurements by the flash photolysis method during the photocycle of the PM, it has been suggested that there are no large changes in the chromophoric transition dipole moments orientations during the bR_{568} to M_{412} transformation (28).

To determine if the out-of-plane orientation angle of the transition dipole moment of the retinal also remained basically unaltered during the bR_{568} to M_{412} transformation under the conditions used for the absorption and CD spectral measurements shown in Figs. 3 and 4, the dichroic ratios were determined from linear dichroic measurements. The orientation angles of the transition dipole moments of the retinals were calculated from the dichroic ratios as previously explained in detail (18). For the bR_{568} species at 568 nm and the M_{412} species at 412 nm, values of 20.9° ± 0.6° and 21.3° ± 0.6°, respectively, were obtained. It is apparent that there has been no observable change in the chromophoric orientation during the species transformation. The only other option left is that the loss of excitonic contributions is due to a loss of the regularity of the chromophoric positions. This is not necessarily indicative of a total loss of the membrane crystal lattice. Excitons are collective excitations that are very intricately dependent on the order of the system in which they are propagated. Loss of this order due to changes ranging from complete lattice destruction to subtle lattice distortions, in which randomization is greater than those imposed by vibronic motions and lattice vibrations, will prevent coupling of the chromophoric transition dipole moments (29). Under these conditions no delocalization of excitations is possible. Therefore, in view of the randomization of the protein orientations in the membrane, during the photocycle it is apparent that the membrane structure is more rigid in the bR_{568} species than in the M_{412} species. This correlates with the results of the time-resolved x-ray diffraction studies of Stamatoff et al. (30) and Frankel and Forsyth (31) that indicated reversible lattice alterations during the photocycle and the electron spin resonance spectral studies of Tokutomi et al. (32) that indicated a transient fluidization of the membrane hydrophobic region during the photocycle. Furthermore, this increase in fluidity of the PM during the photocycle minimizes the role of the native membrane crystallinity in the photoinduced proton translocation function of the membrane. This may provide the answer to why the photochemistry of the PM seems to be essentially monomerlike during the photocycle (33) and why the monomeric bRs seem to be effective proton pumps in artificial lipid vesicles in the absence of the crystalline structure of the PM (34).

Randomization of the chromophoric positions can be in the in-plane or the out-of-plane orientations of the chromophore. However, most likely the randomization is in both since there is no a priori reason for differentiating between those orientations. In fact, if randomization is due to a large scale conformation change of the protein molecules, both orientation modes should be affected. Since the chromophoric out-of-plane angles are nearly the same for the two species as determined by linear dichroism, this limits the heterogeneity of the angle that is possible. For example, if a randomization of the chromophoric positions results in a dispersion in the value of this angle from a nondispersed value of 20° to dispersed values of 10° to 30° in intervals of 0.1°, a simple calculation (based on the relationship given in the Materials and Methods section) shows that the average value of this angle determined by linear dichroism would then be 20.7°. This is well within the experimental uncertainty of the linear dichroic measurements. Therefore, it is apparent that significant randomization in the orientations of the retinals is possible, which would not result in detectable changes in the linear dichroism of the PM.

Near Ultraviolet Spectra

The near UV spectra of PM is mainly due to the π-π^* transition of the three aromatic amino acids, phenylala-

nine, tryptophan, and tryosine. Therefore, spectral changes in this region are indicative of changes in the interactions of the local protein environments with the side chains of these aromatic amino acids and changes in the interactions between these groups. Since ~13% of the amino acids of the bR polypeptide chains are aromatic and the primary structure of the protein indicates that they are fairly uniformly distributed along the chain, the near-UV spectra of PM reflect features of the secondary, tertiary, and quaternary structure of the membrane protein (7, 8). There are also contributions from the higher energy π-π^* transitions of the chromophoric retinal. The near-UV absorption spectra comparing the spectra of the bR_{568} and M_{412} species of the PM in solution and in oriented film are shown in Figs. 1 and 3, respectively. The experimental conditions used for these studies were identical to the ones used for the visible spectral studies. In both spectra species transformation results in small absorbance changes in this spectral region. Due to the relative insensitivity of absorbance, as compared with CD, to protein conformational changes, information concerning such changes abstracted from absorption spectra are uncertain and limited in scope. CD spectra provide a more effective means for obtaining such information. The solution CD spectra of the two species, under the same conditions used for the absorption spectral studies, are compared in Fig. 5. Species transformation resulted in dynamic changes of the ellipticities throughout the entire spectral region as previously reported (22, 23). Furthermore, there has been a fourfold increase in the ellipticity of the weak negative band located at ~285 nm. In addition, a new strong negative band has become apparent at ~295 nm. The spectral changes in the wavelength region 250 to 270 nm are basically the same as previously observed during the bleaching of the PM in the presence of hydroxylamine and during the irreversible denaturing of the PM at pH >12 (14, 16). However, in the region 270 to 300 nm, where the changes due to bleaching and high pH denaturing of the PM are minimal, the changes due to species transformation are maximal. These large changes in the near-UV CD are in contrast to the extremely small changes observed during the dark-light adaptation of the PM and the reversible pH perturbation of the PM in the pH range 2 to 12, which were attributed to localized conformational changes of the protein (13, 16). Furthermore, note that these large changes are in sharp contrast to the lack of detectable changes during the bleaching of the rhodopsin containing bovine rod outer segment membranes (35).

The changes due to species transformation in the 270 to 300-nm region seem to be due to the creation of very specific molecular interactions during the M_{412} formation. Additional details concerning the PM structural changes responsible for these spectral changes can be obtained from oriented CD spectral studies. The film CD spectra of the two species are compared under the same conditions in Fig. 6. It is evident that species transformation results in

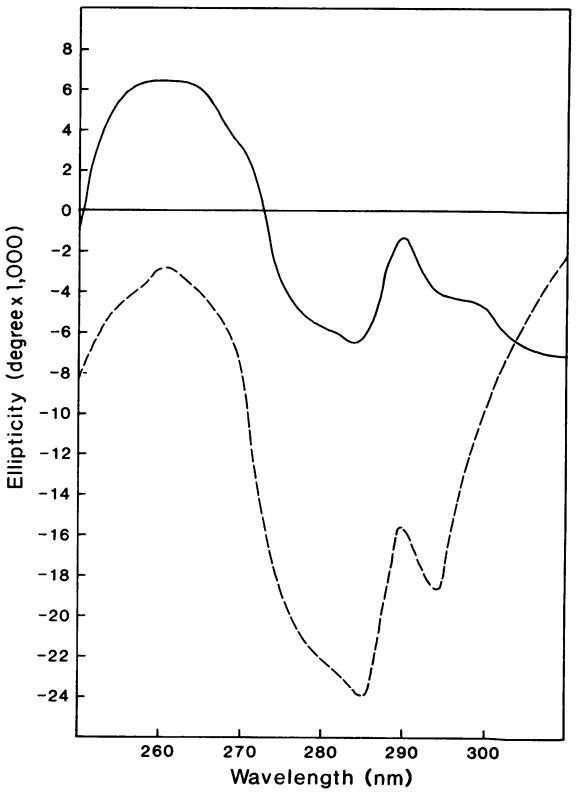

FIGURE 5 Comparative solution circular dichroic spectra of the bR_{568} species (—) and M_{412} species (---) of the purple membrane in the near UV region under the same conditions used for the absorption spectra of Fig. 1. Temperature was −70°C.

significant changes in the orientations of the aromatic amino acids in the PM. Since the aromatic amino acid π-π^* transitions responsible for the near-UV film spectra are polarized in the planes of the aromatic rings of the amino acids, the film spectra reflect the orientations of these rings relative to the membrane plane. The prominent band present at 285 nm in the M_{412} solution spectrum is not present in the film spectrum. This indicates that the planes of the rings of the amino acids that are responsible for this band are oriented nearly perpendicular to the membrane plane. Tryptophans are most likely involved in view of the wavelength of the band maximum and the relatively strong oscillatory strength of tryptophanyl transitions. This is in contrast to the bR_{568} results in which the evidence is in accord with the aromatic rings of the tryptophans lying nearly in the plane of the membrane (15). The strong rotatory strength of this band is suggestive of a strong π-π^* electric-electric dipole coupling. The band apparent at 295 nm in solution is also present in the film spectrum. In view of this and the band position, this band may be attributed to the chromophoric retinal. Free retinal, because of its planar symmetry, is not optically active. The nonexcitonic optical activity of the bR_{568} chromophoric retinal was attributed to the one-electron mechanism by which induced optical activity results from the mixing of wave

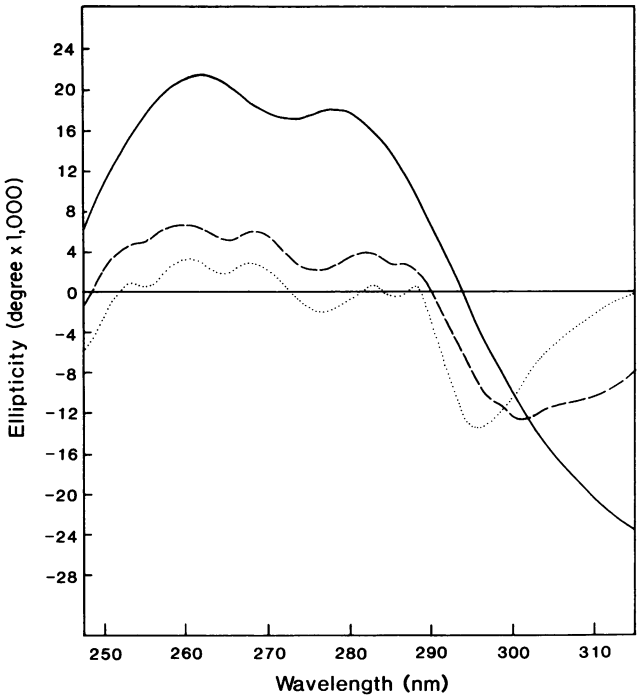

FIGURE 6 Comparative film circular dichroic spectra of the bR_{568} species (—), M_{412} species at 80% conversion (---), and M_{412} species extrapolated to complete conversions (· · ·) of the purple membrane in the near UV region. Temperature was −70°C.

functions of the electrically allowed π-π^* transition of the retinal at 568 nm and the magnetically allowed π-π^* transition of the retinal at 317 nm by an assymmetric charge distribution of the protein (16). In this case, wave functions of the electrically allowed π-π^* transition of the retinal at 412 nm and a possible magnetically allowed π-π^* transition of the retinal at 295 nm would be mixed. This would result in equal and opposite rotatory strength at each frequency. However, the possibility that this band can also be attributed to a coupled-oscillator mechanism by which optical activity is induced from an interaction between the π-π^* transition of the chromophoric retinal at 412 nm and a π-π^* transition of a tryptophanyl aromatic ring at 295 nm cannot be ruled out. In protein CD spectra, tryptophanyl ellipticities are usually indicated by well-resolved peaks at 290–295 nm. However, in view of the 117-nm wavelength difference between these bands the former mechanism is more likely.

A comparison of Figs. 5 and 6 shows that the film and solution spectra of M_{412} are quite different. This result is in contrast to that previously observed in a spectral study of the bR_{568} bleaching process in which the two spectra were nearly identical (15). Furthermore, the study indicated that the anisotropism of bR_{568} membrane structure with respect to the orientations of the aromatic rings of certain amino acid residues to the membrane plane is lost during the bleaching process. However, it is evident from the present study that during the bR_{568} to M_{412} transformation, this structural anisotropism is not lost but altered. A prominent feature of this alteration is the alignment of the planes of some aromatic rings perpendicular to the membrane plane. This alignment so far seems unique to the M_{412} PM structure. It may play a role in the photoinduced vectorial translocation of protons by the membrane in a direction perpendicular to the membrane plane.

Far Ultraviolet Spectra

The far-UV spectrum of the PM is due to the n-π^* and π-π^* transitions of the amide bonds of the protein. Because of this, the CD spectrum in this spectral range serves as a sensitive monitor of the secondary structure of the membrane protein. The solution CD of the PM in the bR_{568} form is shown in Fig. 7. The conditions used were the same as the ones in the other spectral ranges except the membrane protein and salt concentrations were lowered to avoid excessive absorption during CD measurements. However, the concentration ratio of membrane to salt was maintained at the same value as used for the previous measurements. Species transformation resulted in no observable differences in the spectra throughout the entire spectral accessible range 250 to 187 nm. This is indicative of the lack of the significant variance in the net secondary structure of the protein during species transformation. No change was noted during the bleaching of the bR_{568} (14). However, irreversible denaturing of the PM at a pH >12 resulted in significant far-UV spectral changes indicating secondary structural changes (16).

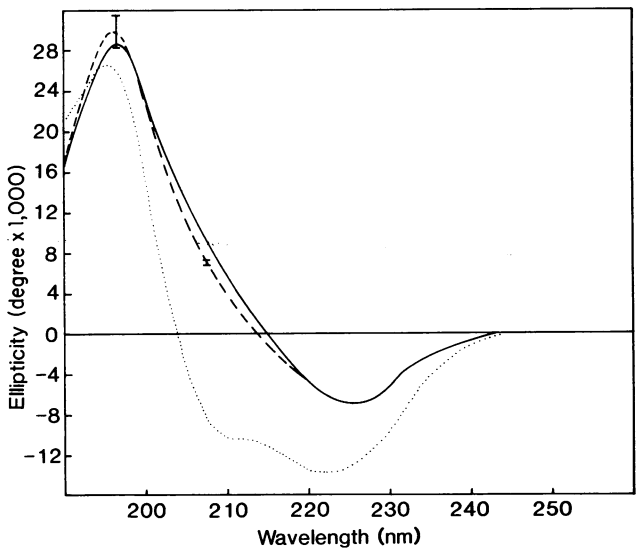

FIGURE 7 Comparative far-UV spectra of bR_{568} in solution (· · ·), bR_{568} in film (—), and M_{412} at 80% conversion in film (---). The spectrum of M_{412} in solution was identical to that of the bR_{568} in solution. Experimental conditions for solution studies: 0.33 M NaCl solution titrated to pH 10 and then mixed with two parts of glycerol; a membrane protein concentration of 5.2 μM and optical pathlength of 0.16 mm (the concentration ratio of protein to NaCl concentration was same as that used in Fig. 1). Temperature was −70°C.

A comparison of the far-UV CD film spectra of the bR_{568} and M_{412} species is also shown in Fig. 7. The M_{412} spectrum is for 80% conversion only. Clearly, there are distinctive spectral changes, albeit small, resulting from the species transformation in the film spectra. The crossover wavelength of the M_{412} spectrum is blue shifted relative to that of the bR_{568} spectrum by ~1.5 nm. Also, there are differences in the ellipticities of the bands. Similar spectral changes have been previously noted during the bleaching and high pH denaturing of the PM (15, 16). These spectral changes are completely reversible for the species transformation and the bleaching cases but not for the high pH denaturing case. In contrast, no changes have been observed in both the solution and the film spectra during dark-light adaptation of the PM and pH perturbation of the PM in the pH range 2 to 12 (13, 16).

Although these spectral changes are small, nevertheless, their analysis may be potentially very important to the elucidation of the proton translocation mechanism of the PM. Cassim and co-workers (15, 16, 24) have previously given a detailed analysis of these changes based on the current spectral theories of polypeptides. A short summary of this analysis is presented again (for details see reference 24 and references cited therein). The far-UV CD of a α-helical proteins consist of three bands: (*a*) a band at 191–193 nm with a net positive rotational strength and corresponding to absorption polarized perpendicular to the helix axis, (*b*) another band at 208–209 nm with a net negative rotational strength and corresponding to absorption polarized parallel to the helix axis, (*c*) and a final band at 222–225 nm with a net negative rotational strength and corresponding to absorption polarized perpendicular to the helix axis. If the protein is oriented so that the helix axis of the protein lies along the direction of the incident light, no absorption polarized parallel to the helix axis is possible. Under these conditions the CD should only consist of the 191–193 nm positive band and the 222–225 nm negative band. Furthermore, the crossover wavelength should drastically red shift relative to the value in the unoriented spectrum. A comparison of the bR_{568} solution and film spectra in Fig. 7 demonstrates these predictable differences in the spectra. The reasons for the ratio of the intensity of the positive and negative band being greater in the film than in the solution spectra has been previously explained and are not essential to the present analysis (15). If the protein helix axes are tilted with respect to the direction of the light propogation, absorption polarized parallel to the helix axis is now possible. Its magnitude will depend on the tilt angle and is maximum at an angle of 90°. The film spectrum will now contain a contribution from the 208–209 nm negative CD band resulting in a blue shift of the crossover wavelength with the extent of the shift depending on the magnitude of the contribution. A shift of the crossover wavelength must result in some change in the ellipticities of the bands also. Therefore, the observed changes in the film spectra are most likely due to significant net tilting of the polypeptide segments during the species transformation. Two other possibilities for such spectral changes, significant changes in the light scattering by the films, and/or mosaic spread from nonuniform stacking of the membrane planes can be ruled out since only results from identical films were compared. Furthermore, no change in film absorbance was observed during species transformation in a transport region such as 800 nm.

The spectrum of proteins oriented randomly with respect to the incident light is an average of the spectra from molecules oriented with the incident light along and perpendicular to the helical axis of the proteins. The perpendicular orientation contributes twice as much as the parallel. Furthermore, when all the protein polypeptide segments are oriented parallel to the direction of light propagation, the ellipticity of the 208-nm CD band should be zero and maximum when they are oriented perpendicular to this direction. Therefore, the maximum ellipticity of the 208-nm CD band should be 1.5 times greater when the segments are perpendicularly oriented than when they are randomly oriented. Randomization of the polypeptide segment orientation to the incident light can be achieved in films by treating bR_{568} films with acetone and subsequently evaporating the acetone with dry nitrogen. No significant change in the protein secondary structure results from this treatment based on solution CD studies. The spectrum of a typical bR_{568} film before and after treatment is compared in Fig. 8. The treated film spectrum resembles a reasonable solution spectrum of bR_{568} with a similar crossover wavelength. Using this spectrum it is possible to make an estimate of the magnitude of the tilt of the polypeptide segments during species transformation from the wavelength shift shown in Fig. 7. Assuming all the polypeptide segments are α-helical, the maximum ellipticity, $(\theta)_{208}$ for the 208-nm band at any tilt angle α is given by $(\theta)_{208} = (\theta)^0_{208} \sin^2 \alpha$, where $(\theta)^0_{208}$ is the maximum ellipicity when α is 90° (that is when segments are oriented parallel to the membrane plane). $(\theta)^0_{208}$ can be approximated as 1.5 times the maximum ellipticity of the 208-nm band of the acetone treated bR_{568} film spectrum (assuming complete randomization of the polypeptide segments). Therefore, assuming that the half-band width of the 208-nm band is independent of tilt angle, the 208-nm band for any angle α can be generated and added to the bR_{568} spectrum (Fig. 7) until a crossover wavelength identical to the one observed in the spectrum of M_{412} (after extrapolating to complete conversion) is achieved. Our calculations indicated an angle of 15° will achieve this. Furthermore, angles <5° resulted in crossover wavelenth changes outside the instrumentation resolving power. Therefore, a conservative estimate of the tilt angle per helical segment is that it lies somewhere between 5 and 15°.

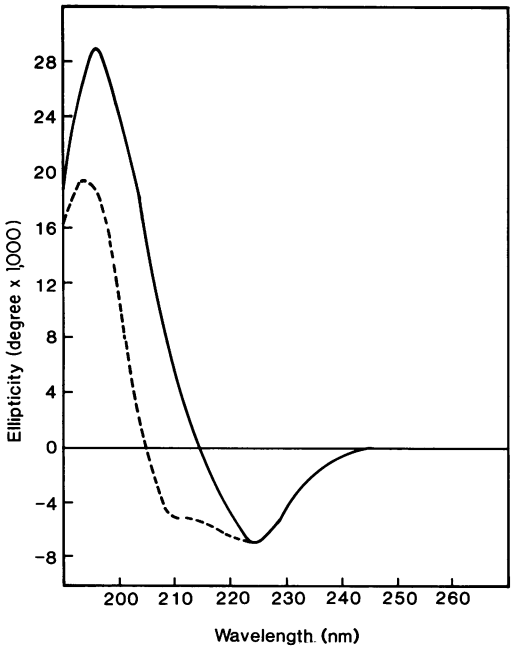

FIGURE 8 Comparative far-UV film spectra of bR_{568}, untreated (—) and treated (---) with acetone. Temperature was −70°C.

Recently, Bagley et al. (36) have concluded from Fourier-transform infrared difference spectroscopic studies based on 30% species transformation that the helical segments are tilted slightly towards and not away from the membrane normal in the bR_{568} to M_{412} transformation. One possible reason for this discrepancy may be due to confusion concerning the nature of the secondary structure of the bR. Estimates of the protein helical content have varied from 45 to 80% depending on the method employed (9, 10, 13). Recently Jap et al. (9) have suggested the possibility of substantial β-sheet in the secondary structure of bR. This possibility will not seriously alter our analysis since the far-UV CD of β-structured proteins is expected to be much less sensitive to protein orientations than that for α-helical proteins. The far-UV CD of β-structured proteins consists of a positive band at ~195 nm, which is the resultant of two close lying bands corresponding to absorption polarized perpendicular and parallel to the chain direction and a negative band at ~217 nm corresponding to absorption polarized perpendicular to the chain direction (37). If the protein chain directions are oriented parallel to the incident light, no major change is expected in the spectrum except minor changes in the relative intensities of the bands. Therefore, if the chain directions are tilted with respect to the incident light in this case, there should be no significant changes in the film spectrum. On the other hand, the presence of substantial β-sheet in the PM will completely alter the analysis of oriented infrared absorption spectra. The contributions of β-sheet structure to the relative absorbances of the amide I and amide II bands of the protein are opposite to those of α-helical structure in similarly oriented spectra. Therefore, a possible alternate analysis of the data of Bagley et al. (36) is that the protein contains both α-helical and β-sheet segments that are tilting away from the membrane normal with the contributions of the β-sheet segments dominating during the bR_{568} to M_{412} transformation. Because of the intersegmental hydrogen bonding of the β-sheet segments, they are expected to tilt more readily in concert than the α-helical ones.

The tilting of the polypeptide segments away from the membrane normal should result in a large scale unfolding of the tertiary structure of the protein. This is consistent with the large changes observed in the near-UV spectra. In view of the hexagonal symmetry of the PM, the unfolding of the protein structure can be correlated with a rotary displacement of the polypeptide segments in all in-plane directions within the membrane crystal lattice resuting in a change of the inclination angle of the segments. In addition, unfolding of the protein structure should change the hydrodynamic characteristics of the protein from a compact one to a less compact one causing an increase in the hydrodynamic size and a change in the protein shape and surface properties. This should lead to distortions of the membrane crystal lattice and randomization of the retinal in-plane and out-of-plane orientations as suggested by the analysis of the visible spectra. Clearly, the structural alterations suggested by analysis of the spectra from each of the spectral regions are consistent. They are in accord with large scale global structural changes of the protein during the photocycle. This apparent amplification of the relatively small conformational distortion of the chromophoric retinal into the relatively large global conformational distortion of the apoprotein may be understood in terms of the inherent metastability of the protein structure. In view of the amino acid sequence and the tertiary structure of the apoprotein, several polar residues may be buried in the hydrophobic interior of the membrane bilayer (7, 8). This molecular geometric arrangement would be highly unstable and strained, somewhat analogous to a wound up spring. A small distortion energy input into this system could result in large distortion energy output.

The nature and extent of these proposed structural changes are not unique. Similar changes have been observed previously in a number of protein systems (for example, see reference 38). An excellent example is the global structural changes induced in the hemoglobin molecule by oxygen binding. A subtle local structural distortion resulting from the binding of oxygen to the heme group of one of the subunits of the hemoglobin molecule is amplified to a large scale global structural change of the entire protein molecule due to the inherent metastability of the protein structure. Furthermore, it is of interest that in this case, as in many others, evidence is in accord with significant tertiary and quaternary structural changes of the

proteins with negligible secondary structure involvement similar to that observed here for the bacteriorhodopsin during the species transformation of the PM.

CONCLUSIONS

The evidence presented in the preceding section is clearly supportive of large scale global structural changes in the purple membrane during the photocycle resulting in the net tilting of the protein polypeptide segments away from the membrane normal. An important consequence of this tilting phenomenon is the possibility of pulsating channels during the photocycle. Previously we suggested that the apparent net tilting of polypeptide segments of the membrane protein during the bleaching process of the PM may result in formation of transmembrane channels perpendicular to the membrane plane. Since no transmembrane channels exist in the native PM, this would explain why the bleached PM is permeable to protons in contrast to the native PM, which blocks their free diffusion (24). Furthermore, this possibility would be in accord with the observations that the bleaching of the PM with hydroxylamine and the reduction of the PM with polar agents cannot be achieved in the dark (2). In view of the similarity of spectral changes during the bleaching and the bR_{568} to M_{412} species transformation of the PM, retinal-regulated channel formation resulting from either process should be equally plausible.

Most importantly, these findings and their consequences bear directly on the fundamental question of how protons are translocated across a hydrophobic membrane bilayer when no apparent channels or pores are present. Based on the highly α-helical nature of transmembrane proteins and their unique orientations in membranes, solid-state protonic semiconductor models have been proposed for membrane proton transport in general and have been applied to the case of the PM (2–4). The essential feature of these models is continuous ordered chains of hydrogen bonds formed from the protein side groups that can serve as proton pathways similar to proton conduction in ice (39). Such extensive intramolecular hydrogen bonding should impart rigidity and conformational stability to the membrane proteins in view of the energy required to form or break such bonds. In contrast, the present study demonstrates the structural metastability of the bR.

A model more consistent with these findings should couple the large scale global structure changes of the PM with the proton translocation process of the membrane. One may visualize the tilting of the rodlike segments of the protein polypeptides during the photocycle to result in a physical pulsating transmembrane channel regulated by the retinal similar to one suggested by Unwin and Zampighi (40) for the gap junction membrane. Protons could be conducted vectorially through such channels in a number of ways, for example, by means of specific aqueous phase ionizable groups transiently situated along the channel. Since transitory aqueous channels would be more kinetic in nature than static, they would not span the entire membrane at any time and thus would avoid the problem of dielectric breakdown inherent in static aqueous channels. On the other hand, perhaps a more realistic view of a pulsating channel considering the time scale involved would be a moving deformation traversing the membrane rather than a physical channel. Therefore, transformation between the structural states of the membrane during the photocycle may give rise to outward and inward deformation waves, which would be the driving force for the proton translocation. Net vectorial translocation of the protons can be accounted for by evoking two pathways in the membrane, differentially resistive to proton movement, coupled to this driving force. Variable stoichiometry would present no problems for this deformation model. Furthermore, this model provides a more universal mechanism for transmembrane transport than the semiconductor models, which are useful at best for transporting protons. Regulated channel mechanisms of this kind based on metastable transmembrane proteins can also be attractive means of transporting a variety of transportable materials by helical transmembrane proteins in general.

Received for publication 14 November 1983 and in final form 29 November 1984.

REFERENCES

1. Eisenbach, M., and S. R. Caplan. 1979. The light-driven proton pump of *Halobacterium halobium:* mechanism and function. *Curr. Top. Membr. Transp.* 12:165–248.
2. Stoeckenius, W., R. H. Lozier, and R. A. Bogomolni. 1979. Bacteriorhodopsin and the purple membrane of Halobacteria. *Biochim. Biophys. Acta.* 505:215–278.
3. Ottolenghi, M. 1980. The photochemistry of rhodopsins. *Adv. Photochem.* 12:97–200.
4. Stoeckenius, W., R. H. Lozier, and R. A. Bogomolni. 1981. Bacteriorhodopsin photocycle and stoichiometry. *In* Chemiosmotic Proton Circuits in Biological Membranes. V. P. Skulachev and P. C. Hinkle, editors. Addison-Wesley Publishing Company, Inc., Reading MA. 283–309.
5. Stoeckenius, W., and R. A. Bogomolni. 1982. Bacteriohodopsin and related pigments of Halobacteria. *Annu. Rev. Biochem.* 51:587–616.
6. Dencher, N. A. 1983. The five retinal protein pigments of *Halobacteria:* bacteriorhodopsin, halorhodopsin, P565, P370 and slow-cycling rhodopsin. *Photochem. Photobiol.* 38:753–767.
7. Khorana, H. G., G. E. Gerber, W. C. Herlihy, C. P. Gray, R. J. Anderegg, K. Nihei, and K. Biemann. 1979. Amino acid sequence of bacteriorhodopsin. *Proc. Natl. Acad. Sci. USA.* 76:5046–5050.
8. Ovchinnikov, Yu A., N. G. Abdulaev, M. Yu. Feignina, A. V. Kiselev, and N. A. Lobanov. 1979. The structural analysis of the functioning bacteriorhodopsin: An overview. *FEBS (Fed. Eur. Biochem. Soc.) Lett.* 100:219–224.
9. Jap, B. K., M. F. Maestre, S. B. Hayward, and R. M. Glaeser. 1983. Peptide-chain secondary structure of bacteriorhodopsin. *Biophys. J.* 43:81–89.
10. Henderson, R. 1977. The purple membrane from *Halobacterium halobium. Annu. Rev. Biophys. Bioeng.* 6:87–109.

11. Lewis, A., J. Spoonhower, R. A. Bogomolni, R. H. Lozier, and W. Stoeckenius. 1974. Tunable laser resonance Raman spectroscopy of bacteriorhodopsin. *Proc. Natl. Acad. Sci. USA.* 71:4462–4466.
12. Oesterhelt, D., M. Meentzen, and L. Schuhmann. 1973. Reversible dissociation of the purple complex of bacteriorhodopsin and identification of 13-*cis* and all-*trans* retinal as its chromophores. *Eur. J. Biochem.* 40:453–463.
13. Becher, B., and J. Y. Cassim. 1976. Effects of light adaptation on the purple membrane structure of *Halobacterium halobium*. *Biophys. J.* 16:1183–1200.
14. Becher, B., and J. Y. Cassim. 1977. Effects of bleaching and regeneration on the purple membrane structure of *Halobacterium halobium*. *Biophys. J.* 19:285–297.
15. Muccio, D. D., and J. Y. Cassim. 1979. Interpretation of the absorption and circular dichroic spectra of oriented purple membrane films. *Biophys. J.* 26:427–440.
16. Muccio, D. D., and J. Y. Cassim. 1979. Interpretations of the effects of pH on the spectra of purple membrane. *J. Mol. Biol.* 135:595–609.
17. Becher, B., and J. Y. Cassim. 1975. Improved isolation procedures for the purple membrane of *Halobacterium halobium*. *Prep. Biochem.* 5:161–178.
18. Becher, B., and T. G. Ebrey. 1977. The quantum efficiency for the photochemical conversion of the purple membrane protein. *Biophys. J.* 17:185–191.
19. Papadopoulos, G. K., and J. Y. Cassim. 1981. Orientations of the retinyl and heme chromophore in the brown membrane. *J. Mol. Biol.* 152:35–47.
20. Stoeckenius, W., and R. H. Lozier. 1974. Light energy conversion in *Halobacterium halobium*. *J. Supramol. Struct.* 2:769–774.
21. Schreckenbach, T., B. Walckhoff, and D. Oesterhelt. 1974. Studies on the retinal-protein interaction in bacteriorhodopsin. *Eur. J. Biochem.* 76:499–511.
22. Heyn, M. P., P.-J. Bauer, and N. A. Dencher. 1975. Natural CD label to probe the structure of the purple membrane from *Halobacterium halobium* by means of exciton coupling effects. *Biochem. Biophys. Res. Commun.* 67:897–903.
23. Yoshida, M., K. Ohno, Y. Takeuchi, and Y. Kagawa. 1977. Prolonged lifetime of the 410 nm intermediate of bacteriorhodopsin in the presence of guanidine hydrochloride. *Biochem. Biophys. Res. Commun.* 75:1111–1116.
24. Papadopoulos, G. K., and J. Y. Cassim. 1981. Interpretations of the solution and oriented film spectra of brown membrane. *Photochem. Photobiol.* 33:455–466.
25. Draheim, J. E., and J. Y. Cassim. 1983. Effects of polyhydric alcohols on the structure of purple membrane. *Biophys. J.* (2, Pt. 2):331*a*. (Abstr.)
26. Muccio, D. D., and J. Y. Cassim. 1981. Analysis of the spectroscopic properties of bacteriorhodopsin in the purple membrane by a crystalline exciton model. *Biophys. J.* 33(2, Pt. 2):103*a*. (Abstr.)
27. Ebrey, T. G., B. Becher, B. Mao, P. Kilbride, and B. Honig. 1977. Exciton interactions and chromophore orientation in the purple membrane. *J. Mol. Biol.* 112:377–397.
28. Czege, J., A. Dér, L. Zimaniyi, and L. Keszthelyi. 1982. Restriction of motion of protein side chains during the photocycle of bacteriorhodopsin. *Proc. Natl. Acad. Sci. USA.* 79:7273–7277.
29. Craig, D. P., and S. H. Walmsley. 1968. Excitons in Molecular Crystals: Theory and Applications. W. A. Benjamin, Inc., New York.
30. Stamatoff, J., R. Lozier, G. King, and W. Stoeckenius. 1980. Photoinduced structural changes of purple membranes. *Fed. Proc.* 39:1849. (Abstr.)
31. Frankel, R. D., and J. M. Forsyth. 1983. Time resolved x-ray diffraction studies of purple membrane from *Halobacterium halobium*. *Biophys. J.* 41(2, Pt. 2):15*a*. (Abstr.)
32. Tokutomi, S., T. Iwasa, T. Yoshizawa, and S. Ohnishi. 1981. Flash-induced change in surface potential and fluidity of purple membrane studied by spin label method. *Photochem. Photobiol.* 33:467–474.
33. El-Sayed, M. A., B. Karvaly, and J. M. Fukumoto. 1981. Primary step in the bacteriorhodopsin photocycle: Photochemistry or exiton transfer? *Proc. Natl. Acad. Sci. USA.* 78:7512–7516.
34. Dencher, N. A., and M. P. Heyn. 1979. Bacteriorhodopsin monomers pump protons. *FEBS (Fed. Eur. Biochem. Soc.) Lett.* 198:307–310.
35. Rafferty, C. N., J. Y. Cassim, and D. G. McConnell. 1977. Circular dichroism, optical rotatory dispersion and absorption studies on the conformation of bovine rhodopsin in situ and solubilized with detergent. *Biophys. Struct. Mechanism.* 2:277–320.
36. Bagley, K., G. Dollinger, L. Eisenstein, A. K. Singh, and L. Zimaniyi. 1982. Fourier transform infrared difference spectroscopy of bacteriorhodopsin and its photoproducts. *Proc. Natl. Acad. Sci. USA.* 79:4972–4976.
37. Sears, D. W. and S. Beychok. 1973. Circular dichroism. *In* Physical Principles and Techniques of Protein Chemistry. Part C. S. J. Leach, editor. Academic Press, Inc., New York. 445–593.
38. Perutz, M. F., and L. F. TenEyck. 1971. Stereochemistry of cooperative effects in hemoglobin. *Cold Spring Harbor Symp. Quant. Biol.* 36:295–310.
39. Onsager, L. 1973. Physics and Chemistry of Ice. E. Whalley, editor. Royal Society, Canada. 7–12.
40. Unwin, P. N. T., and G. Zampighi. 1980. Structure of the junction between communicating cells. *Nature (Lond.).* 283:545–549.